

# Boundary adaptive observer design for semilinear hyperbolic rolling contact ODE-PDE systems with uncertain friction

Luigi Romano<sup>\*a,b,c</sup>, Ole Morten Aamo<sup>b</sup>, Miroslav Krstić<sup>c</sup>, Jan Aslund<sup>a</sup>, and Erik Frisk<sup>a</sup>

<sup>a</sup>Department of Electrical Engineering, Linköping University, SE-581 83 Linköping, Sweden

<sup>b</sup>Department of Engineering Cybernetics, Norwegian University of Science and Technology, O. S. Bragstads plass 2, NO-7034, Trondheim, Norway

<sup>c</sup>Department of Mechanical and Aerospace Engineering, University of California San Diego, La Jolla, CA, 92093, USA

## Abstract

This paper presents an adaptive observer design for semilinear hyperbolic rolling contact ODE-PDE systems with uncertain friction characteristics parameterized by a matrix of unknown coefficients appearing in the nonlinear (and possibly non-smooth) PDE source terms. Under appropriate assumptions of forward completeness and boundary sensing, an adaptive observer is synthesized to simultaneously estimate the lumped and distributed states, as well as the uncertain friction parameters, using only boundary measurements. The observer combines a finite-dimensional parameter estimator with an infinite-dimensional description of the state error dynamics, and achieves exponential convergence under persistent excitation. The effectiveness of the proposed design is demonstrated in simulation by considering a relevant example borrowed from road vehicle dynamics.

## 1 Introduction

Rolling contact systems with spatially-distributed friction effects arise in numerous mechanical applications, such as vehicle dynamics [1–6], rotating machinery [7, 8], and robotic locomotion [9]. A common modeling approach involves interconnecting finite-dimensional ordinary differential equations (ODEs), which represent the rigid body dynamics, with hyperbolic partial differential equations (PDEs) that describe the behavior of the contact interface, in the presence of dry or lubricated friction [10, 11]. In many engineering applications, particularly in the automotive domain, accurately estimating system states and physical parameters is essential not only for real-time control but also for monitoring, diagnostics, and higher-level functions. For example, retrieving the tire-road friction coefficient is critical not only for the design of Advanced Driver Assistance Systems (ADAS), such as anti-lock braking systems (ABS) and electronic stability control (ESC) [12], but also for road condition characterization, which may enhance safety, efficiency, and coordination of both individual vehicles and entire fleets [13, 14].

Motivated by these considerations, this paper addresses the problem of joint state and parameter estimation for a class of semilinear, homodirectional ODE-PDE systems. These systems model rolling contact dynamics with distributed friction, where the PDE subsystem features nonlinear source terms governed by unknown parameters, and couples to the ODE dynamics through integral function-

als of the distributed state and, possibly, boundary terms. The proposed observer reconstructs both the lumped and distributed states, as well as the friction-related parameters, using only boundary measurements. Importantly, in contrast to classical adaptive control frameworks where parameter estimation serves the primary goal of stabilizing or regulating the system, the focus here is on accurate estimation per se. This distinction reflects application scenarios in which reliable state and parameter reconstruction is valuable in its own right, independent of any direct control objective.

Adaptive observer design for PDE systems initially emerged within the broader framework of adaptive output-feedback control, particularly for parabolic PDEs [15]. This foundational approach was later extended to first-order hyperbolic integro-differential equations with unknown functional coefficients in [16], and to more general heterodirectional hyperbolic systems featuring both boundary and in-domain parametric uncertainties in [17]. In [18], the disturbance rejection problem for coupled ODE-2 × 2 hyperbolic systems was also addressed, albeit without parameter uncertainties. However, in many of these early developments, particularly those embedded in adaptive output-feedback controllers, convergence of the estimated parameters to their true values is not always guaranteed or even required. In contrast, a growing line of research has shifted focus toward adaptive observers aimed specifically at accurate estimation of both the system states and unknown parameters, independently of any control objective. Within this direction, which aligns with the scope of the present paper, adaptive

<sup>\*</sup>Corresponding author. Email: luigi.romano@liu.se.

observers have been developed for  $2 \times 2$  hyperbolic systems in [19], wave equations with in-domain uncertainties in [20], and general  $n+1$  and  $n+m$  hyperbolic PDEs in [21, 22].

Concerning coupled hyperbolic ODE-PDE systems with unknown parameters, notable works include those of [23], which consider a  $2 \times 2$  hyperbolic PDE coupled with an uncertain linear time-invariant (LTI) ODE, [19], which analyzes a class of linear homodirectional hyperbolic PDEs coupled with uncertain linear time-varying (LTV) ODEs, and [24, 25], where the sources of uncertainty appear in the PDE subsystem. Most of these studies, however, are limited to linear, heterodirectional systems. With notable exceptions for the non-adaptive case (see, e.g., [26]), the extension to semilinear equations, possibly homodirectional and with unknown parameters, also remains limited. The challenge lies in the nonlinearity of the PDE, the finite-dimensional nature of the parameter estimation problem, and the need to preserve well-posedness and convergence guarantees. The problem becomes even more delicate when considering ODE-PDE interconnections with nonlinear and non-differentiable coefficients, as is the case in the present paper, where friction-related terms introduce sources of non-smoothness.

Building upon recent advances in adaptive control and PDE estimation ([27, 28]), a novel observer architecture is proposed that combines a finite-dimensional adaptive law for parameter estimation based on filtered regression equations with an infinite-dimensional observer driven by boundary measurements. The approach establishes exponential convergence under mild assumptions on the system dynamics and excitation properties of the inputs. The mathematical analysis is based on standard Lyapunov arguments, similar to those utilized in [29], in conjunction with uniform convergence results obtained for a regularized version of the non-smooth problem considered in the paper. The proposed framework is validated considering a vehicle model with Dahl-type distributed tire friction, showing fast and robust convergence of both state and parameter estimates.

The remainder of this manuscript is organized as follows. Section 2 introduces the problem formulation and the underlying hypotheses needed for observer design. Section 3 first presents a finite-dimensional adaptive law for parameter estimation, and then proceeds to the synthesis of the adaptive observer for the system's states. Section 4 illustrates an application of the proposed methodology to a relevant example from vehicle dynamics, whereas Section 5 concludes with final remarks.

## Notation

In this paper,  $\mathbb{R}$  denotes the set of real numbers;  $\mathbb{R}_{>0}$  and  $\mathbb{R}_{\geq 0}$  indicate the set of positive real numbers excluding and including zero, respectively;  $\mathbb{N}_0$  indicates the set of integers including zero. The set of  $n \times m$  matrices with values in  $\mathbb{F}$  ( $\mathbb{F} = \mathbb{R}$ ,  $\mathbb{R}_{>0}$ , or  $\mathbb{R}_{\geq 0}$ ) is denoted by  $\mathbf{M}_{n \times m}(\mathbb{F})$  (abbreviated as  $\mathbf{M}_n(\mathbb{F})$  whenever  $m = n$ ).  $\mathbf{GL}_n(\mathbb{F})$  and  $\mathbf{Sym}_n(\mathbb{F})$  represents the groups of invertible and symmetric matrices, respectively, with values in  $\mathbb{F}$ ; the identity matrix on  $\mathbb{R}^n$  is indicated with  $I_n$ . A positive-definite matrix is noted as  $\mathbf{M}_n(\mathbb{R}) \ni Q \succ 0$ . The identity operator on a Banach space  $\mathcal{Z}$  is denoted by  $I_{\mathcal{Z}}$ . The standard Euclidean norm on  $\mathbb{R}^n$

is indicated with  $\|\cdot\|_2$ ; operator norms are simply denoted by  $\|\cdot\|$ .  $L^2((0, 1); \mathbb{R}^n)$  denotes the Hilbert space of square-integrable functions on  $(0, 1)$  with values in  $\mathbb{R}^n$ , endowed with inner product  $\langle \zeta_1, \zeta_2 \rangle_{L^2((0, 1); \mathbb{R}^n)} = \int_0^1 \zeta_1^T(\xi) \zeta_2(\xi) d\xi$  and induced norm  $\|\zeta(\cdot)\|_{L^2((0, 1); \mathbb{R}^n)}$ . The Hilbert space  $H^1((0, 1); \mathbb{R}^n)$  consists of functions  $\zeta \in L^2((0, 1); \mathbb{R}^n)$  whose weak derivative also belongs to  $L^2((0, 1); \mathbb{R}^n)$ ; it is naturally equipped with norm  $\|\zeta(\cdot)\|_{H^1((0, 1); \mathbb{R}^n)}^2 \triangleq \|\zeta(\cdot)\|_{L^2((0, 1); \mathbb{R}^n)}^2 + \left\| \frac{\partial \zeta(\cdot)}{\partial \xi} \right\|_{L^2((0, 1); \mathbb{R}^n)}^2$ . Given a domain  $\Omega$  with closure  $\overline{\Omega}$ ,  $L^p(\Omega; \mathcal{Z})$  and  $C^k(\overline{\Omega}; \mathcal{Z})$  ( $p, k \in \{1, 2, \dots, \infty\}$ ) denote respectively the spaces of  $L^p$ -integrable functions and  $k$ -times continuously differentiable functions on  $\overline{\Omega}$  with values in  $\mathcal{Z}$  (for  $T = \infty$ , the interval  $[0, T]$  is identified with  $\mathbb{R}_{\geq 0}$ ). Given two Hilbert spaces  $\mathcal{V}$  and  $\mathcal{W}$ ,  $\mathcal{L}(\mathcal{V}; \mathcal{W})$  denotes the spaces of linear operators from  $\mathcal{V}$  to  $\mathcal{W}$  (abbreviated  $\mathcal{L}(\mathcal{V})$  if  $\mathcal{V} = \mathcal{W}$ ). Finally, following [30], the group of operators on a Banach space  $\mathcal{Z}$  that are infinitesimal generators of a  $C_0$ -semigroup satisfying  $\|T(t)\| \leq e^{\omega t}$  is conventionally denoted by  $\mathcal{G}(\mathcal{Z}; 1, \omega)$ .

## 2 Problem statement

This section is dedicated to introducing the considered ODE-PDE system, along with the main assumptions formulated about its structure and the available measurements.

### 2.1 Structure of the considered ODE-PDE system

In this paper, the following semilinear homodirectional hyperbolic ODE-PDE interconnection is considered:

$$\begin{aligned} \dot{X}(t) &= A_1 X(t) + G_1(\mathcal{K}_1 z)(t) + G_1 \Theta \Sigma(v(X(t), U(t))) (\mathcal{K}_2 z)(t) \\ &\quad + G_1 h_1(v(X(t), U(t))), \quad t \in (0, T), \end{aligned} \tag{1a}$$

$$\begin{aligned} \frac{\partial z(\xi, t)}{\partial t} + \Lambda \frac{\partial z(\xi, t)}{\partial \xi} &= \Theta \Sigma(v(X(t), U(t))) z(\xi, t) \\ &\quad + h_2(v(X(t), U(t))), \quad (\xi, t) \in (0, 1) \times (0, T), \end{aligned} \tag{1b}$$

$$z(0, t) = 0, \quad t \in (0, T), \tag{1c}$$

where  $X(t) \in \mathbb{R}^{n_x}$  indicates the lumped state vector,  $z(\xi, t) \in \mathbb{R}^{n_z}$  denotes the distributed state vector,  $U(t) \in \mathbb{R}^{n_u}$  represents the input to the PDE subsystem,  $\mathbf{Sym}_{n_z}(\mathbb{R}) \ni \Theta = \text{diag}\{\theta_1, \dots, \theta_{n_z}\} \succ 0$  is a diagonal matrix of unknown parameters, and the rigid relative velocity  $v \in C^1(\mathbb{R}^{n_x+n_u}; \mathbb{R}^{n_z})$  reads

$$v(X, U) = A_2 X + G_2 U. \tag{2}$$

In (1) and (2), the matrix  $\mathbf{GL}_{n_z}(\mathbb{R}) \cap \mathbf{Sym}_{n_z}(\mathbb{R}) \ni \Lambda = \text{diag}\{\lambda_1, \dots, \lambda_{n_z}\} \succ 0$  collects the transport velocities,  $\Sigma \in C^0(\mathbb{R}^{n_z}; \mathbf{M}_{n_z}(\mathbb{R}))$  represents the nonlinear source matrix, the matrices  $A_1 \in \mathbf{M}_{n_x}(\mathbb{R})$ ,  $A_2 \in \mathbf{M}_{n_z \times n_x}(\mathbb{R})$ ,  $G_1 \in$

$\mathbf{M}_{n_X \times n_z}(\mathbb{R})$ , and  $G_2 \in \mathbf{M}_{n_z \times n_U}(\mathbb{R})$  have constant coefficients,  $h_1 \in C^0(\mathbb{R}^{n_z}; \mathbb{R}^{n_z})$ , and  $h_2 \in C^0(\mathbb{R}^{n_z}; \mathbb{R}^{n_z})$  is invertible. Finally, the operators  $(\mathcal{K}_1\zeta)$  and  $(\mathcal{K}_2\zeta)$  satisfy  $\mathcal{K}_1 \in \mathcal{L}(H^1((0, 1); \mathbb{R}^{n_z}); \mathbb{R}^{n_z})$  and  $\mathcal{K}_2 \in \mathcal{L}(L^2((0, 1); \mathbb{R}^{n_z}); \mathbb{R}^{n_z})$ , and are given by

$$(\mathcal{K}_1\zeta) \triangleq \int_0^1 K_1(\xi)\zeta(\xi) d\xi + K_2\zeta(1), \quad (3a)$$

$$(\mathcal{K}_2\zeta) \triangleq \int_0^1 K_3(\xi)\zeta(\xi) d\xi, \quad (3b)$$

with  $K_1, K_3 \in C^0([0, 1]; \mathbf{M}_{n_z}(\mathbb{R}))$ , and  $K_2 \in \mathbf{M}_{n_z}(\mathbb{R})$ .

ODE-PDE interconnections of the type (1) typically describe rolling contact systems where the lumped states capture the rigid body dynamics, and the distributed ones describe the rolling contact motion in the presence of dry or lubricated friction. For instance, distributed friction models that can be put in the form (1b) are the Dahl model, the LuGre model [10], and certain variants of the FrBD model recently developed in [11]. From a mathematical perspective, the ODE-PDE interconnection (1) is (locally) well-posed. In particular, the Hilbert spaces  $\mathcal{X} \triangleq \mathbb{R}^{n_X} \times L^2((0, 1); \mathbb{R}^{n_z})$  and  $\mathcal{Y} \triangleq \mathbb{R}^{n_X} \times H^1((0, 1); \mathbb{R}^{n_z})$  are considered, equipped respectively with norms  $\|(Z, \zeta(\cdot))\|_{\mathcal{X}}^2 \triangleq \|Z\|_2^2 + \|\zeta(\cdot)\|_{L^2((0, 1); \mathbb{R}^{n_z})}^2$  and  $\|(Z, \zeta(\cdot))\|_{\mathcal{Y}}^2 \triangleq \|Z\|_2^2 + \|\zeta(\cdot)\|_{H^1((0, 1); \mathbb{R}^{n_z})}^2$ , along with the domain  $\mathcal{D}(\mathcal{A}) \triangleq \{(Z, \zeta) \in \mathcal{Y} \mid \zeta(0) = 0\}$ . With the above definitions, local well-posedness is enounced by Theorem 2.1 below.

**Theorem 2.1** (Local existence and uniqueness of solutions). *Suppose that  $\Sigma \in C^0(\mathbb{R}^{n_z}; \mathbf{M}_{n_z}(\mathbb{R}))$  and  $h_1, h_2 \in C^0(\mathbb{R}^{n_z}; \mathbb{R}^{n_z})$  are locally Lipschitz continuous, and  $U \in C^0([0, T]; \mathbb{R}^{n_U})$ . Then, for all initial conditions (ICs)  $(X_0, z_0) \triangleq (X(0), z(\cdot, 0)) \in \mathcal{X}$ , there exists  $t_{\max} \leq \infty$  such that the ODE-PDE system (1) admits a unique mild solution  $(X, z) \in C^0([0, t_{\max}); \mathcal{X})$ . Additionally, if  $\Sigma \in C^1(\mathbb{R}^{n_z}; \mathbf{M}_{n_z}(\mathbb{R}))$ ,  $h_1, h_2 \in C^1(\mathbb{R}^{n_z}; \mathbb{R}^{n_z})$ , and  $U \in C^1([0, T]; \mathbb{R}^{n_U})$ , for all ICs  $(X_0, z_0) \in \mathcal{D}(\mathcal{A})$ , the solution is classical, i.e.,  $(X, z) \in C^1([0, t_{\max}); \mathcal{X}) \cap C^0([0, t_{\max}); \mathcal{D}(\mathcal{A}))$ .*

*Proof.* The proof is similar to that of Theorems 3.1 and 3.2 in [31], and hence omitted for brevity.  $\square$

Theorem 2.1 merely asserts local existence and uniqueness results for the solutions of (1). In the following, it is explicitly assumed that the input  $U \in L^\infty(\mathbb{R}_{\geq 0}; \mathbb{R}^{n_U})$  is such that the existence of such solutions is global, so that  $t_{\max} = \infty$ , and moreover that the solution of (1) remains uniformly bounded in time in an appropriate spatial norm (alternatively, global existence and uniqueness may be guaranteed by enforcing more stringent conditions on the structure of the nonlinear terms appearing in (1), see Theorem 3.3 in [31] and related hypotheses). These assumptions are better formalized below.

**Assumption 2.1** (Forward completeness and boundedness). *The ODE-PDE system (1) is forward complete, that is,  $t_{\max} = \infty$  in Theorem 2.1. Moreover,  $(X, z) \in L^\infty(\mathbb{R}_{\geq 0}; \mathcal{X})$  for mild solutions,  $(X, z) \in L^\infty(\mathbb{R}_{\geq 0}; \mathcal{Y})$  for classical solutions, and  $U \in L^\infty(\mathbb{R}_{\geq 0}; \mathbb{R}^{n_U})$ .*

Under Assumption 2.1, the scope of this paper consists of reconstructing the parameters contained in the matrix  $\Theta$ , and the lumped and distributed states, using only boundary measurements from the PDE subsystem (1b), as clarified in the next Section 2.2. In this context, it is worth clarifying that the assumption that all friction-related information is fully captured by the matrix  $\Theta$  is standard in the literature ([13, 14, 32]). Other model parameters are typically slowly varying and can therefore be identified either non-adaptively or through linearized versions of (1).

In the following, convergence results for the error dynamics will be asserted in two different norms ( $\|\cdot\|_{\mathcal{X}}$  and  $\|\cdot\|_{\mathcal{Y}}$ , respectively), depending on the smoothness of the matrix-valued function  $\Sigma(\cdot)$  figuring in (1). Indeed, for  $\Sigma \in C^0(\mathbb{R}^{n_z}; \mathbf{M}_{n_z}(\mathbb{R}))$  and  $h_1, h_2 \in C^0(\mathbb{R}^{n_z}; \mathbb{R}^{n_z})$  locally Lipschitz, Theorem 2.1 only guarantees the existence and uniqueness of mild solutions, which motivates studying the convergence of the observer error dynamics in the norm  $\|\cdot\|_{\mathcal{X}}$ . Conversely,  $\Sigma \in C^1(\mathbb{R}^{n_z}; \mathbf{M}_{n_z}(\mathbb{R}))$  and  $h_1, h_2 \in C^1(\mathbb{R}^{n_z}; \mathbb{R}^{n_z})$  permit recovering classical solutions and consequently stronger estimates for the observer error dynamics, whose convergence may be studied in the norm  $\|\cdot\|_{\mathcal{Y}}$ . Despite the intrinsic non-smooth nature of friction, the case with  $\Sigma \in C^1(\mathbb{R}^{n_z}; \mathbf{M}_{n_z}(\mathbb{R}))$  and  $h_1, h_2 \in C^1(\mathbb{R}^{n_z}; \mathbb{R}^{n_z})$  is considered for completeness. This is also motivated by the widespread use of regularized friction models in engineering practice, as extensively documented in the literature [33–35].

## 2.2 Assumptions and considerations on the available measurements

Concerning the measured signals, two sets of measurements are supposed to be available: the first is needed for the design of a non-adaptive observer, whereas the second facilitates the synthesis of the adaptive one. Both types of signals considered in this paper may be acquired, as is typically the case, using accelerometers or strain gauges mounted on the rolling contact components. As these sensors rotate with the mechanical elements, they capture state variations in the Lagrangian reference frame, yielding direct measurements of true accelerations and velocities. In contrast, the PDE (1b) is formulated in the Eulerian framework. The relationship between the Lagrangian and Eulerian time derivatives is given by

$$\frac{dz(\xi, t)}{dt} = \frac{\partial z(\xi, t)}{\partial t} + \Lambda \frac{\partial z(\xi, t)}{\partial \xi}. \quad (4)$$

Starting with (4), the first set of measurements is defined as

$$Y_1(t) = \frac{dz(0, t)}{dt} = \Lambda \frac{\partial z(0, t)}{\partial \xi} = h_2(v(X(t), U(t))), \quad (5)$$

giving

$$v(X(t), U(t)) = h_2^{-1}(Y_1(t)). \quad (6)$$

Equations (5) and (6) permits reconstructing the rigid relative velocity directly from available measurements. Accordingly, the following assumption is formulated.

**Assumption 2.2** (Detectability). *The pair  $(A_1, A_2)$  is detectable.*

The second set of measurements is instead defined as

$$\begin{aligned} Y_2(t) &= \frac{d^2z(0, t)}{dt^2} \\ &= \Lambda\Theta\Sigma\left(v(X(t), U(t))\right)\frac{\partial z(0, t)}{\partial\xi} + \dot{h}_2\left(v(X(t), U(t))\right) \\ &= \Theta\Lambda\Sigma\left(h_2^{-1}(Y_1(t))\right)\Lambda^{-1}Y_1(t) + \dot{Y}_1(t), \end{aligned} \quad (7)$$

where the fact that  $\Lambda$  and  $\Theta$  commute has been used.

Before moving to the design of an adaptive observer, some considerations are formalized in Remark 1 below.

**Remark 1.** *As indicated by (5) and (7), acquiring the full set of  $2n_z$  measurements may initially seem like a stringent requirement. However, in most practical cases, certain components of  $X(t)$  are readily accessible, enabling the recovery of the rigid relative velocity  $v(X(t), U(t))$  by observing only a single component of the PDE subsystem. Moreover, the number of unknown parameters in the matrix  $\Theta$  can often be reduced, which in turn decreases the dimensionality of  $Y_2(t)$ . Nevertheless, to present a simple, general, and compact framework for joint parameter and state estimation focused exclusively on boundary sensing, this paper assumes that the full set of  $2n_z$  measurements is available.*

### 3 Adaptive observer design

The present section addresses the synthesis of an adaptive observer design for the ODE-PDE system (1), assuming that the friction parameters contained in the matrix  $\Theta$  are uncertain. Specifically, Section 3.1 derives a finite-dimensional adaptive law for parameter identification, whereas Section 3.2 is dedicated to the design of the observer, delivering the main result of the paper.

#### 3.1 Parameter identifiers and adaptive laws

The first step consists of deriving a suitable adaptive law to estimate the unknown parameters contained in the matrix  $\Theta$ . The ODE-based approach adopted in this paper is partly inspired from [27], and makes only use of finite-dimensional tools. In particular, defining the vector  $\mathbb{R}^{n_z} \ni 1_{n_z} \triangleq [1 \dots 1]^T$ , and introducing the variables

$$\begin{aligned} Z_1(t) &\triangleq 1_{n_z}^T Y_1(t), \quad Z_2(t) \triangleq 1_{n_z}^T Y_2(t), \quad \theta \triangleq \Theta 1_{n_z}, \\ \phi(t) &\triangleq -\Lambda\Sigma\left(h_2^{-1}(Y_1(t))\right)\Lambda^{-1}Y_1(t), \end{aligned} \quad (8)$$

a linear parametric model may be derived as

$$\dot{Z}_1(t) = \theta^T \phi(t) + Z_2(t). \quad (9)$$

The following filters may now be designed:

$$\dot{\zeta}_1(t) = -\varrho(\zeta_1(t) - Z_1(t)), \quad (10a)$$

$$\dot{\zeta}_2(t) = -\varrho\zeta_2(t) + Z_2(t), \quad (10b)$$

$$\dot{\phi}(t) = -\varrho\phi(t) + \phi(t), \quad t \in (0, T), \quad (10c)$$

for some gain  $\varrho \in \mathbb{R}_{>0}$ . Accordingly, the non-adaptive estimate  $\bar{Z}_1(t) \in \mathbb{R}$  of  $Z_1(t)$  may be generated from

$$\bar{Z}_1(t) = \theta^T \varphi(t) + \zeta(t), \quad (11)$$

with  $\mathbb{R} \ni \zeta(t) \triangleq \zeta_1(t) + \zeta_2(t)$ . It should be noted that  $(X, z) \in C^0([0, T]; \mathcal{X})$  implies that  $\bar{Z}_1, \zeta \in C^0([0, T]; \mathbb{R})$  and  $\varphi \in C^0([0, T]; \mathbb{R}^{n_z})$ , ensuring that the signals in (11) are well-defined for both mild and classical solutions of (1). Formally, the dynamics of the non-adaptive state error  $\mathbb{R} \ni \tilde{Z}_1(t) \triangleq Z_1(t) - \bar{Z}_1(t)$  may be easily deduced to obey

$$\dot{\tilde{Z}}_1(t) = -\varrho\tilde{Z}_1(t), \quad t \in (0, T). \quad (12)$$

At this point, any standard adaptive law may be employed to estimate the parameters in  $\theta$ , as explained in [36]. Below, the gradient law with integral cost function is stated. In the following, the estimate of  $\theta$  is denoted as  $\hat{\theta}(t) \in \mathbb{R}^{n_z}$ , whereas the parameter estimation error as  $\mathbb{R}^{n_z} \ni \tilde{\theta}(t) \triangleq \theta - \hat{\theta}(t)$ .

**Theorem 3.1.** *Suppose that  $U \in C^0([0, T]; \mathbb{R}^{n_U})$ , and consider the ODE-PDE interconnection (1), with measurements (5) and (7), and filters (10). If Assumption 2.1 holds, the adaptive law*

$$\dot{\hat{\theta}}(t) = -\Gamma(R(t)\hat{\theta}(t) + Q(t)), \quad t \in (0, T), \quad (13)$$

where  $\mathbf{Sym}_{n_z}(\mathbb{R}) \ni \Gamma \succ 0$ , and

$$\dot{R}(t) = -\psi R(t) + \frac{\varphi(t)\varphi^T(t)}{1 + \|\varphi(t)\|_2^2}, \quad (14a)$$

$$\dot{Q}(t) = -\psi Q(t) - \frac{(Z_1(t) - \zeta(t))\varphi(t)}{1 + \|\varphi(t)\|_2^2}, \quad t \in (0, T), \quad (14b)$$

with  $R(t) \in \mathbf{M}_{n_z}(\mathbb{R})$ ,  $Q(t) \in \mathbb{R}^{n_z}$ , and  $\psi \in \mathbb{R}_{>0}$ , ensures that

$$\tilde{\theta} \in L^\infty(\mathbb{R}_{\geq 0}; \mathbb{R}^{n_z}), \quad (15a)$$

$$\tilde{Z}_1 \in L^\infty(\mathbb{R}_{\geq 0}; \mathbb{R}) \times L^2(\mathbb{R}_{>0}; \mathbb{R}), \quad (15b)$$

$$\dot{\hat{\theta}} \in L^\infty(\mathbb{R}_{\geq 0}; \mathbb{R}^{n_z}) \times L^2(\mathbb{R}_{>0}; \mathbb{R}^{n_z}), \quad (15c)$$

$$\lim_{t \rightarrow \infty} \left\| \dot{\hat{\theta}}(t) \right\|_2 = 0. \quad (15d)$$

Moreover, if  $\varphi \in L^\infty(\mathbb{R}_{\geq 0}; \mathbb{R})$  in (10c) is persistently exciting (PE), then  $\left\| \tilde{\theta}(t) \right\|_2 \rightarrow 0$  exponentially fast.

*Proof.* See [36]. □

An estimate of the matrix  $\Theta$  may thus be constructed as  $\mathbf{Sym}_{n_z}(\mathbb{R}) \ni \hat{\Theta}(t) = \text{diag}\{\hat{\theta}_1(t), \dots, \hat{\theta}_{n_z}(t)\}$ , so that  $\mathbf{Sym}_{n_z}(\mathbb{R}) \ni \tilde{\Theta}(t) \triangleq \Theta - \hat{\Theta}(t) = \text{diag}\{\tilde{\theta}_1(t), \dots, \tilde{\theta}_{n_z}(t)\}$ . In this context, it should also be emphasized that (13) and (14), in conjunction with (8) and (10), imply that  $\hat{\theta}, \tilde{\Theta} \in C^1(\mathbb{R}_{\geq 0}; \mathbf{Sym}_{n_z}(\mathbb{R}))$ . Obviously  $\left\| \hat{\Theta}(t) \right\| \leq \left\| \hat{\theta}(t) \right\|_2$  and  $\left\| \tilde{\Theta}(t) \right\| \leq \left\| \tilde{\theta}(t) \right\|_2$ , and hence from (15a) it immediately follows that

$$\left\| \hat{\Theta} \right\|, \left\| \tilde{\Theta} \right\| \in L^\infty(\mathbb{R}_{\geq 0}; \mathbf{Sym}_{n_z}(\mathbb{R})). \quad (16)$$

Additionally,  $\|\tilde{\Theta}(t)\| \rightarrow 0$  exponentially fast whenever  $\varphi \in L^\infty(\mathbb{R}_{\geq 0}; \mathbb{R})$  in (10c) is PE. Owing to these premises, it is possible to proceed with the synthesis of an adaptive observer to estimate the lumped and distributed states. This is the objective of the next Section 3.2.

### 3.2 Adaptive observer

Denoting the estimates of  $X(t)$ ,  $z(\xi, t)$ , and  $Y_1(t)$  respectively as  $\hat{X}(t) \in \mathbb{R}^{n_x}$ ,  $\hat{z}(\xi, t) \in \mathbb{R}^{n_z}$ , and  $\hat{Y}_1(t) \in \mathbb{R}^{n_z}$ , the following observer structure is proposed:

$$\begin{aligned} \dot{\hat{X}}(t) &= A_1 \hat{X}(t) + G_1(\mathcal{K}\hat{z})(t) \\ &+ G_1 \hat{\Theta}(t) \Sigma(h_2^{-1}(Y_1(t))) (\mathcal{K}_2 \hat{z})(t) + G_1 h_1(h_2^{-1}(Y_1(t))) \\ &- L_1(h_2^{-1}(Y_1(t)) - h_2^{-1}(\hat{Y}_1(t))), \quad t \in (0, T), \end{aligned} \quad (17a)$$

$$\begin{aligned} \frac{\partial \hat{z}(\xi, t)}{\partial t} + \Lambda \frac{\partial \hat{z}(\xi, t)}{\partial \xi} &= \hat{\Theta}(t) \Sigma(h_2^{-1}(Y_1(t))) \hat{z}(\xi, t) + Y_1(t) \\ &(\xi, t) \in (0, 1) \times (0, T), \end{aligned} \quad (17b)$$

$$\hat{z}(0, t) = 0, \quad t \in (0, T), \quad (17c)$$

where  $L_1 \in \mathbf{M}_{n_X \times n_z}(\mathbb{R})$  is a matrix with constant coefficients. The estimated output reads

$$\hat{Y}_1(t) = h_2(v(\hat{X}(t), U(t))) = h_2(A_2 \hat{X}(t) + G_2 U(t)). \quad (18)$$

Consequently, defining the error variables as  $\mathbb{R}^{n_X} \ni \tilde{X}(t) \triangleq X(t) - \hat{X}(t)$  and  $\mathbb{R}^{n_z} \ni \tilde{z}(\xi, t) \triangleq z(\xi, t) - \hat{z}(\xi, t)$ , and subtracting (17) from (1), the observer error dynamics is governed by

$$\begin{aligned} \dot{\tilde{X}}(t) &= A_1 \tilde{X}(t) + G_1(\mathcal{K}\tilde{z})(t) \\ &+ G_1 \hat{\Theta}(t) \Sigma(v(X(t), U(t))) (\mathcal{K}_2 \tilde{z})(t) \\ &+ G_1 \tilde{\Theta}(t) \Sigma(v(X(t), U(t))) (\mathcal{K}_2 z)(t) \\ &+ L_1(h_2^{-1}(Y_1(t)) - h_2^{-1}(\hat{Y}_1(t))), \quad t \in (0, T), \end{aligned} \quad (19a)$$

$$\begin{aligned} \frac{\partial \tilde{z}(\xi, t)}{\partial t} + \Lambda \frac{\partial \tilde{z}(\xi, t)}{\partial \xi} &= \hat{\Theta}(t) \Sigma(v(X(t), U(t))) \tilde{z}(\xi, t) \\ &+ \tilde{\Theta}(t) \Sigma(v(X(t), U(t))) z(\xi, t), \\ &(\xi, t) \in (0, 1) \times (0, T), \end{aligned} \quad (19b)$$

$$\tilde{z}(0, t) = 0, \quad t \in (0, T), \quad (19c)$$

where

$$h_2^{-1}(Y_1(t)) - h_2^{-1}(\hat{Y}_1(t)) = v(\tilde{X}(t), 0) = A_2 \tilde{X}(t). \quad (20)$$

Recalling Assumption 2.2,  $L_1$  may be chosen such that  $\mathbf{M}_{n_X}(\mathbb{R}) \ni \bar{A}_1 \triangleq A_1 + L_1 A_2$  is Hurwitz. Thus, the observer error dynamics (19) becomes

$$\begin{aligned} \dot{\tilde{X}}(t) &= \bar{A}_1 \tilde{X}(t) + G_1(\mathcal{K}_1 \tilde{z})(t) + F_1(t) (\mathcal{K}_2 \tilde{z})(t) \\ &+ f_1(t), \quad t \in (0, T), \end{aligned} \quad (21a)$$

$$\begin{aligned} \frac{\partial \tilde{z}(\xi, t)}{\partial t} + \Lambda \frac{\partial \tilde{z}(\xi, t)}{\partial \xi} &= F_2(t) \tilde{z}(\xi, t) + f_2(\xi, t), \\ &(\xi, t) \in (0, 1) \times (0, T), \end{aligned} \quad (21b)$$

$$\tilde{z}(0, t) = 0, \quad t \in (0, T), \quad (21c)$$

where

$$F_1(t) \triangleq G_1 \hat{\Theta}(t) \Sigma(v(X(t), U(t))), \quad (22a)$$

$$F_2(t) \triangleq \hat{\Theta}(t) \Sigma(v(X(t), U(t))), \quad (22b)$$

and

$$f_1(t) \triangleq G_1 \tilde{\Theta}(t) \Sigma(v(X(t), U(t))) (\mathcal{K}_2 \tilde{z})(t), \quad (23a)$$

$$f_2(\xi, t) \triangleq \tilde{\Theta}(t) \Sigma(v(X(t), U(t))) \tilde{z}(\xi, t). \quad (23b)$$

Assumption 2.1 ensures that  $(X, z) \in C^0(\mathbb{R}_{\geq 0}; \mathcal{X}) \cap L^\infty(\mathbb{R}_{\geq 0}; \mathcal{X})$  and  $U \in C^0(\mathbb{R}_{\geq 0}; \mathbb{R}^{n_U}) \cap L^\infty(\mathbb{R}_{\geq 0}; \mathbb{R}^{n_U})$ , which, combined with  $\hat{\Theta}, \tilde{\Theta} \in C^1(\mathbb{R}_{\geq 0}; \mathbf{Sym}_{n_z}(\mathbb{R})) \cap L^\infty(\mathbb{R}_{\geq 0}; \mathbf{Sym}_{n_z}(\mathbb{R}))$ , implies that  $F_1 \in C^0(\mathbb{R}_{\geq 0}; \mathbf{M}_{n_X \times n_z}(\mathbb{R})) \cap L^\infty(\mathbb{R}_{\geq 0}; \mathbf{M}_{n_X \times n_z}(\mathbb{R}))$ ,  $F_2 \in C^0(\mathbb{R}_{\geq 0}; \mathbf{M}_{n_z}(\mathbb{R})) \cap L^\infty(\mathbb{R}_{\geq 0}; \mathbf{M}_{n_z}(\mathbb{R}))$ ,  $f_1 \in C^0(\mathbb{R}_{\geq 0}; \mathbb{R}^{n_X}) \cap L^\infty(\mathbb{R}_{\geq 0}; \mathbb{R}^{n_X})$ , and  $f_2 \in C^0(\mathbb{R}_{\geq 0}; L^2((0, 1); \mathbb{R}^{n_z})) \cap L^\infty(\mathbb{R}_{\geq 0}; L^2((0, 1); \mathbb{R}^{n_z}))$ . Thus, similar arguments as those in the proof of Theorem 2.1 yield the existence of a unique (global) mild solution  $(\tilde{X}, \tilde{z}) \in C^0(\mathbb{R}_{\geq 0}; \mathcal{X})$  to (21) for all ICs  $(\tilde{X}_0, \tilde{z}_0) \triangleq (\tilde{X}(0), \tilde{z}(\cdot, 0)) \in \mathcal{X}$ . However, since  $\Sigma(\cdot)$  is only supposed to be continuous in its argument, classical solutions to the ODE-PDE system (21) are not guaranteed by Theorem 2.1.

Therefore, for  $n \in \mathbb{N}_0$ , the following regularized version of the ODE-PDE system (21) is also considered:

$$\begin{aligned} \dot{\tilde{X}}^n(t) &= \bar{A}_1 \tilde{X}^n(t) + G_1(\mathcal{K}_1 \tilde{z}^n)(t) + F_1^n(t) (\mathcal{K}_2 \tilde{z}^n)(t) \\ &+ f_1^n(t), \quad t \in (0, T), \end{aligned} \quad (24a)$$

$$\begin{aligned} \frac{\partial \tilde{z}^n(\xi, t)}{\partial t} + \Lambda \frac{\partial \tilde{z}^n(\xi, t)}{\partial \xi} &= F_2^n(t) \tilde{z}^n(\xi, t) + f_2^n(\xi, t), \\ &(\xi, t) \in (0, 1) \times (0, T), \end{aligned} \quad (24b)$$

$$\tilde{z}^n(0, t) = 0, \quad t \in (0, T), \quad (24c)$$

where  $F_1^n \in C^1(\mathbb{R}_{\geq 0}; \mathbf{M}_{n_X \times n_z}(\mathbb{R})) \cap L^\infty(\mathbb{R}_{\geq 0}; \mathbf{M}_{n_X \times n_z}(\mathbb{R}))$ ,  $F_2^n \in C^1(\mathbb{R}_{\geq 0}; \mathbf{M}_{n_z}(\mathbb{R})) \cap L^\infty(\mathbb{R}_{\geq 0}; \mathbf{M}_{n_z}(\mathbb{R}))$ ,  $f_1^n \in C^1(\mathbb{R}_{\geq 0}; \mathbb{R}^{n_X}) \cap L^\infty(\mathbb{R}_{\geq 0}; \mathbb{R}^{n_X})$ , and  $f_2^n \in C^1(\mathbb{R}_{\geq 0}; L^2((0, 1); \mathbb{R}^{n_z})) \cap L^\infty(\mathbb{R}_{\geq 0}; L^2((0, 1); \mathbb{R}^{n_z}))$  satisfy

$$F_1^n \xrightarrow{n \rightarrow \infty} F_1, \quad \text{in } L^\infty(\mathbb{R}_{\geq 0}; \mathbf{M}_{n_X \times n_z}(\mathbb{R})), \quad (25a)$$

$$F_2^n \xrightarrow{n \rightarrow \infty} F_2, \quad \text{in } L^\infty(\mathbb{R}_{\geq 0}; \mathbf{M}_{n_z}(\mathbb{R})), \quad (25b)$$

$$f_1^n \xrightarrow{n \rightarrow \infty} f_1, \quad \text{in } L^\infty(\mathbb{R}_{\geq 0}; \mathbb{R}^{n_X}), \quad (25c)$$

$$f_2^n \xrightarrow{n \rightarrow \infty} f_2, \quad \text{in } L^\infty(\mathbb{R}_{\geq 0}; L^2((0, 1); \mathbb{R}^{n_z})). \quad (25d)$$

Similar arguments as those in the proof of Theorem 2.1 ensure the existence of a unique (global) classical solution  $(\tilde{X}^n, \tilde{z}^n) \in C^1(\mathbb{R}_{\geq 0}; \mathcal{X}) \times C^0(\mathbb{R}_{\geq 0}; \mathcal{D}(\mathcal{A}))$  to (24) for all ICs  $(\tilde{X}_0^n, \tilde{z}_0^n) \triangleq (\tilde{X}^n(0), \tilde{z}^n(\cdot, 0)) \in \mathcal{D}(\mathcal{A})$ .

Lemma 3.1 below is propaedeutic to deriving the main result of this section.

**Lemma 3.1.** Consider the mild solution  $(\tilde{X}, \tilde{z}) \in C^0([0, T]; \mathcal{X})$  of (21), along with the classical solution  $(\tilde{X}^n, \tilde{z}^n) \in C^1([0, T]; \mathcal{X}) \cap C^0([0, T]; \mathcal{D}(\mathcal{A}))$  of (24). Then, for all and  $(X, z) \in C^0(\mathbb{R}_{\geq 0}; \mathcal{X}) \cap L^\infty(\mathbb{R}_{\geq 0}; \mathcal{X})$ ,  $U \in C^0(\mathbb{R}_{\geq 0}; \mathbb{R}^{n_U}) \cap L^\infty(\mathbb{R}_{\geq 0}; \mathbb{R}^{n_U})$  and  $\hat{\Theta}, \tilde{\Theta} \in C^1(\mathbb{R}_{\geq 0}; \mathbf{Sym}_{n_z}(\mathbb{R})) \cap L^\infty(\mathbb{R}_{\geq 0}; \mathbf{Sym}_{n_z}(\mathbb{R}))$ , and ICs  $(\tilde{X}_0, \tilde{z}_0) \in \mathcal{X}$  and  $(\tilde{X}_0^n, \tilde{z}_0^n) \in \mathcal{D}(\mathcal{A})$  satisfying

$$(\tilde{X}_0^n, \tilde{z}_0^n) \xrightarrow[n \rightarrow \infty]{} (\tilde{X}_0, \tilde{z}_0), \quad \text{in } \mathcal{X}, \quad (26)$$

there exists  $\omega_\rho \in \mathbb{R}_{>0}$  such that

$$\sup_{t \in \mathbb{R}_{\geq 0}} e^{-\omega_\rho t} \|(\tilde{X}(t), \tilde{z}(\cdot, t)) - (\tilde{X}^n(t), \tilde{z}^n(\cdot, t))\|_{\mathcal{X}} \xrightarrow[n \rightarrow \infty]{} 0. \quad (27)$$

*Proof.* See Appendix A.  $\square$

**Theorem 3.2.** Suppose that  $\Sigma \in C^0(\mathbb{R}^{n_z}; \mathbf{M}_{n_z}(\mathbb{R}))$ ,  $h_1, h_2 \in C^0(\mathbb{R}^{n_z}; \mathbb{R}^{n_z})$  are locally Lipschitz continuous, and  $U \in C^0([0, T]; \mathbb{R}^{n_U})$ , and consider the mild solutions  $(X, z), (\tilde{X}, \tilde{z}) \in C^0([0, T]; \mathcal{X})$  of (1) and (21), respectively, together with the adaptive law (13) and (14). Then, if Assumptions 2.1 and 2.2 hold,  $(\tilde{X}, \tilde{z}) \in L^\infty(\mathbb{R}_{\geq 0}; \mathcal{X})$ . Moreover, if  $\varphi \in L^\infty(\mathbb{R}_{\geq 0}; \mathbb{R})$  in (10c) is PE,  $\|(\tilde{X}(t), \tilde{z}(\cdot, t))\|_{\mathcal{X}} \rightarrow 0$  exponentially fast.

*Proof.* The strategy consists of proving the result for the regularized ODE-PDE system (24), for whose classical solutions a suitable energy estimate may be derived using standard Lyapunov arguments. Resorting to (27), the obtained bound is then extended to mild solutions of (21). To this end, the following Lyapunov function candidate is considered:

$$\begin{aligned} V(\tilde{X}^n(t), \tilde{z}^n(\cdot, t)) &\triangleq \frac{1}{2} \tilde{X}^{n\top}(t) P \tilde{X}^n(t) \\ &\quad + \frac{\gamma}{2} \int_0^1 e^{-\alpha \xi} \tilde{z}^{n\top}(\xi, t) \tilde{z}^n(\xi, t) d\xi, \end{aligned} \quad (28)$$

for a positive definite matrix  $\mathbf{Sym}_{n_X}(\mathbb{R}) \ni P \succ 0$  and constants  $\alpha, \gamma \in \mathbb{R}_{>0}$  to be appropriately specified.

Taking the derivative of (28) along the dynamics (24) yields

$$\begin{aligned} \dot{V}(t) &= \frac{1}{2} \tilde{X}^{n\top}(t) \left( \bar{A}_1^\top P + P \bar{A}_1 \right) \tilde{X}^n(t) + \tilde{X}^{n\top}(t) P f_1^n(t) \\ &\quad + \tilde{X}^{n\top}(t) P [G_1(\mathcal{K}_1 \tilde{z}^n)(t) + F_1^n(t)(\mathcal{K}_2 \tilde{z}^n)(t)] \\ &\quad - \gamma \int_0^1 e^{-\alpha \xi} \tilde{z}^{n\top}(\xi, t) \Lambda \frac{\partial \tilde{z}^n(\xi, t)}{\partial \xi} d\xi \\ &\quad + \gamma \int_0^1 e^{-\alpha \xi} \tilde{z}^{n\top}(\xi, t) F_2^n(t) \tilde{z}^n(\xi, t) d\xi \\ &\quad + \gamma \int_0^1 e^{-\alpha \xi} \tilde{z}^{n\top}(\xi, t) f_2^n(\xi, t) d\xi, \quad t \in (0, T). \end{aligned} \quad (29)$$

Assumption 2.2 implies that the matrix  $P$  may be selected such that  $\bar{A}_1^\top P + P \bar{A}_1 = -2pI_{n_X}$ , with  $p \in \mathbb{R}_{>0}$  arbitrarily large. Moreover, integrating by parts the fourth term in (29)

and using the BC (24c) provides

$$\begin{aligned} \dot{V}(t) &= -p \left\| \tilde{X}^n(t) \right\|_2^2 + \tilde{X}^{n\top}(t) P f_1^n(t) \\ &\quad + \tilde{X}^{n\top}(t) P [G_1(\mathcal{K}_1 \tilde{z}^n)(t) + F_1^n(t)(\mathcal{K}_2 \tilde{z}^n)(t)] \\ &\quad - \frac{\gamma}{2} e^{-\alpha t} \tilde{z}^{n\top}(1, t) \Lambda \tilde{z}^n(1, t) \\ &\quad - \frac{\gamma \alpha}{2} \int_0^1 e^{-\alpha \xi} \tilde{z}^{n\top}(\xi, t) \Lambda \tilde{z}^n(\xi, t) d\xi \\ &\quad + \gamma \int_0^1 e^{-\alpha \xi} \tilde{z}^{n\top}(\xi, t) F_2^n(t) \tilde{z}^n(\xi, t) d\xi \\ &\quad + \gamma \int_0^1 e^{-\alpha \xi} \tilde{z}^{n\top}(\xi, t) f_2^n(\xi, t) d\xi, \quad t \in (0, T). \end{aligned} \quad (30)$$

From (3), it may also be inferred that there exist  $\eta_1, \eta_2 \in \mathbb{R}_{>0}$  such that

$$(\mathcal{K}_1 \tilde{z}^n)(t) \leq \eta_1 (\| \tilde{z}^n(\cdot, t) \|_{L^2((0,1); \mathbb{R}^{n_z})} + \| \tilde{z}^n(1, t) \|_2), \quad (31a)$$

$$(\mathcal{K}_2 \tilde{z}^n)(t) \leq \eta_2 \| \tilde{z}^n(\cdot, t) \|_{L^2((0,1); \mathbb{R}^{n_z})}. \quad (31b)$$

Moreover, by virtue of (22) and (25), there exist  $\eta_3, \eta_4 \in \mathbb{R}_{>0}$  such that

$$\| F_1(\cdot) \|_\infty, \| F_1^n(\cdot) \|_\infty \leq \eta_3, \quad (32a)$$

$$\| F_2(\cdot) \|_\infty, \| F_2^n(\cdot) \|_\infty \leq \eta_4, \quad n \in \mathbb{N}_0. \quad (32b)$$

Consequently, the first two cross terms appearing in (30) may be bounded as

$$\tilde{X}^{n\top}(t) P f_1^n(t) \leq \frac{p}{4} \left\| \tilde{X}^n(t) \right\|_2^2 + \frac{\| P \|^2}{p} \| f_1^n(t) \|_2^2, \quad (33a)$$

$$\begin{aligned} \tilde{X}^{n\top}(t) P [G_1(\mathcal{K}_1 \tilde{z}^n)(t) + F_1^n(t)(\mathcal{K}_2 \tilde{z}^n)(t)] &\leq \frac{p}{4} \left\| \tilde{X}^n(t) \right\|_2^2 \\ &\quad + \frac{2\| P \|^2 \eta_5^2}{p} \left( \| \tilde{z}^n(\cdot, t) \|_{L^2((0,1); \mathbb{R}^{n_z})}^2 + \| \tilde{z}^n(1, t) \|_2^2 \right), \end{aligned} \quad (33b)$$

with  $\mathbb{R}_{>0} \ni \eta_5 \triangleq \| G_1 \| \eta_1 + \eta_2 \eta_3$ . Similarly, the last two cross terms in (30) may be bounded as

$$\begin{aligned} &\int_0^1 e^{-\alpha \xi} \tilde{z}^{n\top}(\xi, t) F_2^n(t) \tilde{z}^n(\xi, t) d\xi \\ &\leq \eta_4 \int_0^1 e^{-\alpha \xi} \| \tilde{z}^n(\xi, t) \|_2^2 d\xi, \end{aligned} \quad (34a)$$

$$\begin{aligned} &\int_0^1 e^{-\alpha \xi} \tilde{z}^{n\top}(\xi, t) f_2^n(\xi, t) d\xi \\ &\leq \frac{\alpha \lambda_{\min}(\Lambda)}{4} \int_0^1 e^{-\alpha \xi} \| \tilde{z}^n(\xi, t) \|_2^2 d\xi \end{aligned} \quad (34b)$$

$$+ \frac{1}{\alpha \lambda_{\min}(\Lambda)} \| f_2^n(\cdot, t) \|_{L^2((0,1); \mathbb{R}^{n_z})}^2,$$

with  $\mathbb{R}_{>0} \ni \lambda_{\min}(\Lambda)$  denoting the smallest eigenvalue of  $\Lambda$ . Combining (33), (34), and (30), and selecting  $\alpha \in \mathbb{R}_{>0}$  satisfying  $\alpha > \frac{2\eta_4}{\lambda_{\min}(\Lambda)}$  ensures the existence of  $\eta_6 \in \mathbb{R}_{>0}$

such that

$$\begin{aligned}
\dot{V}(t) = & -\frac{p}{2} \left\| \tilde{X}^n(t) \right\|_2^2 + \frac{\|P\|^2}{p} \left\| f_1^n(t) \right\|_2^2 \\
& - \left( \frac{\gamma}{2} \lambda_{\min}(\Lambda) e^{-\alpha} - \frac{2\|P\|^2 \eta_5^2}{p} \right) \left\| \tilde{z}^n(1, t) \right\|_2^2 \\
& - \left( \frac{\gamma \eta_6}{2} - \frac{2\|P\|^2 \eta_5^2}{p} \right) \left\| \tilde{z}^n(\cdot, t) \right\|_{L^2((0,1); \mathbb{R}^{n_z})}^2 \\
& + \frac{\gamma}{\alpha \lambda_{\min}(\Lambda)} \left\| f_2^n(\cdot, t) \right\|_{L^2((0,1); \mathbb{R}^{n_z})}^2, \quad t \in (0, T).
\end{aligned} \tag{35}$$

Hence, choosing  $\gamma \in \mathbb{R}_{>0}$  sufficiently large implies the existence of constants  $\bar{\omega}, \eta \in \mathbb{R}_{>0}$  such that

$$\dot{V}(t) \leq -\bar{\omega} V(t) + \eta \left\| f^n(\cdot, t) \right\|_{\mathcal{X}}^2, \quad t \in (0, T), \tag{36}$$

with  $\mathbb{R}^{n_x+n_z} \ni f^n(\xi, t) \triangleq [f_1^n(t) \ f_2^n(t)]^T$ . Thus, applying Grönwall-Bellman's inequality and observing that the Lyapunov function  $V(X^n(t), \tilde{z}^n(\cdot, t))$  is equivalent to the squared norm  $\left\| (\tilde{X}^n(t), \tilde{z}^n(\cdot, t)) \right\|_{\mathcal{X}}^2$  on  $\mathcal{X}$  provides

$$\begin{aligned}
\left\| (\tilde{X}^n(t), \tilde{z}^n(\cdot, t)) \right\|_{\mathcal{X}} & \leq \beta_1 e^{-\sigma t} \left\| (\tilde{X}_0^n, \tilde{z}_0^n(\cdot)) \right\|_{\mathcal{X}} \\
& + \beta_2 \sqrt{\int_0^t e^{-\bar{\omega}(t-t')} \left\| f^n(\cdot, t') \right\|_{\mathcal{X}}^2 dt'}, \quad t \in [0, T],
\end{aligned} \tag{37}$$

for some  $\beta_1, \beta_2, \sigma \in \mathbb{R}_{>0}$ . Finally, recalling (27), letting  $n \rightarrow \infty$  in (37), and invoking the lower-semicontinuity property of the norms together with the Dominated Convergence Theorem produces

$$\begin{aligned}
\left\| (\tilde{X}(t), \tilde{z}(\cdot, t)) \right\|_{\mathcal{X}} & \leq \beta_1 e^{-\sigma t} \left\| (\tilde{X}_0, \tilde{z}_0(\cdot)) \right\|_{\mathcal{X}} \\
& + \beta_2 \sqrt{\int_0^t e^{-\bar{\omega}(t-t')} \left\| f(\cdot, t') \right\|_{\mathcal{X}}^2 dt'}, \quad t \in [0, T],
\end{aligned} \tag{38}$$

where  $\mathbb{R}^{n_x+n_z} \ni f(\xi, t) \triangleq [f_1^T(t) \ f_2^T(\xi, t)]^T$ . The conclusion follows immediately from the bound (38), in conjunction with the assumed behavior of  $\left\| f(\cdot, t) \right\|_{\mathcal{X}}$ , which is dictated by that of  $z(\xi, t)$ ,  $(\mathcal{K}_2 z)(t)$ , and  $\tilde{\Theta}(t)$ .  $\square$

**Theorem 3.3.** Suppose that  $\Sigma \in C^1(\mathbb{R}^{n_z}; \mathbf{M}_{n_z}(\mathbb{R}))$ ,  $h_1, h_2 \in C^1(\mathbb{R}^{n_z}; \mathbb{R}^{n_z})$ , and  $U \in C^1([0, T]; \mathbb{R}^{n_u})$ , and consider the classical solutions  $(X, z), (\tilde{X}, \tilde{z}) \in C^1([0, T]; \mathcal{X}) \cap C^0([0, T]; \mathcal{D}(\mathcal{A}))$  of (1) and (21), respectively, together with the adaptive law (13) and (14). Then, if Assumptions 2.1 and 2.2 hold,  $(\tilde{X}, \tilde{z}) \in L^\infty(\mathbb{R}_{\geq 0}; \mathcal{Y})$ . Moreover, if  $\varphi \in L^\infty(\mathbb{R}_{\geq 0}; \mathbb{R})$  in (10c) is PE,  $\left\| (\tilde{X}(t), \tilde{z}(\cdot, t)) \right\|_{\mathcal{Y}} \rightarrow 0$  exponentially fast.

*Proof.* If  $\Sigma \in C^1(\mathbb{R}^{n_z}; \mathbf{M}_{n_z}(\mathbb{R}))$ ,  $h_1 \in C^1(\mathbb{R}^{n_z}; \mathbb{R}^{n_x})$ ,  $h_2 \in C^1(\mathbb{R}^{n_z}; \mathbb{R}^{n_z})$ , and  $U \in C^1([0, T]; \mathbb{R}^{n_u})$ , the observer error dynamics (21) indeed admits a unique (global) classical solution  $(\tilde{X}, \tilde{z}) \in C^1(\mathbb{R}_{\geq 0}; \mathcal{X}) \cap C^0(\mathbb{R}_{\geq 0}; \mathcal{D}(\mathcal{A}))$ . Therefore, the bound (38) may be derived by considering directly the Lyapunov function  $V(\tilde{X}(t), \tilde{z}(\cdot, t))$  defined according to (28), implying that  $(\tilde{X}, \tilde{z}) \in L^\infty(\mathbb{R}_{\geq 0}; \mathcal{X})$ , and

$\left\| (\tilde{X}(t), \tilde{z}(\cdot, t)) \right\|_{\mathcal{X}} \rightarrow 0$  exponentially fast whenever  $\varphi \in L^\infty(\mathbb{R}_{\geq 0}; \mathbb{R})$  in (10c) is PE. Additionally, defining  $\mathbb{R}^{n_z} \ni \tilde{\zeta}(\xi, t) \triangleq \frac{\partial \tilde{z}(\xi, t)}{\partial \xi}$  and taking the partial derivative of (21b) yields

$$\begin{aligned}
\frac{\partial \tilde{\zeta}(\xi, t)}{\partial t} + \Lambda \frac{\partial \tilde{\zeta}(\xi, t)}{\partial \xi} & = F_2(t) \tilde{\zeta}(\xi, t) + f_3(\xi, t), \\
(\xi, t) & \in (0, 1) \times (0, T),
\end{aligned} \tag{39a}$$

$$\tilde{\zeta}(0, t) = 0, \quad t \in (0, T), \tag{39b}$$

with

$$f_3(\xi, t) \triangleq \frac{\partial f_2(\xi, t)}{\partial \xi} = \tilde{\Theta}(t) \left( v(X(t), U(t)) \right) \frac{\partial z(\xi, t)}{\partial \xi}. \tag{40}$$

In conjunction with Assumption 2.1,  $(X, z) \in C^1(\mathbb{R}_{\geq 0}; \mathcal{X}) \cap C^0(\mathbb{R}_{\geq 0}; \mathcal{D}(\mathcal{A}))$  implies that  $f_3 \in C^0(\mathbb{R}_{\geq 0}; \mathcal{X}) \cap L^\infty(\mathbb{R}_{\geq 0}; \mathcal{X})$ .

Hence, for classical solutions of (39), using standard Lyapunov arguments, it is possible to derive an energy estimate of the form

$$\begin{aligned}
\left\| \tilde{\zeta}(\cdot, t) \right\|_{L^2((0,1); \mathbb{R}^{n_z})} & \leq \beta_3 e^{-\sigma' t} \left\| \tilde{\zeta}_0(\cdot) \right\|_{L^2((0,1); \mathbb{R}^{n_z})} \\
& + \beta_4 \sqrt{\int_0^t e^{-\bar{\omega}'(t-t')} \left\| f_3(\cdot, t') \right\|_{L^2((0,1); \mathbb{R}^{n_z})}^2 dt'}, \quad t \in [0, T],
\end{aligned} \tag{41}$$

for some  $\beta_3, \beta_4, \bar{\omega}', \sigma' \in \mathbb{R}_{>0}$ . The above bound (41) may be extended to mild solutions of (39) following a similar rationale as that adopted in the proof of Lemma 3.1. The conclusion is an immediate consequence of the estimate (41) and the definition of  $\tilde{\zeta}(\xi, t)$ .  $\square$

Theorem 3.3 concludes the technical part of the paper. Before moving to Section 4, it is worth remarking that Theorems 3.2 and 3.3 require PE conditions for the signal  $\varphi(t)$  to ensure the convergence of the observer error dynamics in the corresponding norms. In practice, PE conditions need to be checked numerically; preliminary insights on how to design the control input  $U(t)$  to ensure PE of  $\varphi(t)$  may also be gained by employing reduced-order representations of the ODE-PDE system (1), see, e.g., [37].

## 4 An example from road vehicle dynamics

The proposed adaptive observer is validated considering a relevant example borrowed from vehicle dynamics. The next Section 4.1 introduces the model equations, whereas Section 4.2 presents the simulation results.

### 4.1 Lateral vehicle dynamics

The performance of the adaptive observer designed in Section 3.2 is tested on a semilinear single-track model governing the lateral dynamics of a road vehicle driving at a constant cruising speed. A schematic of the model is depicted in Figure 1. In particular, for sufficiently small steering in-

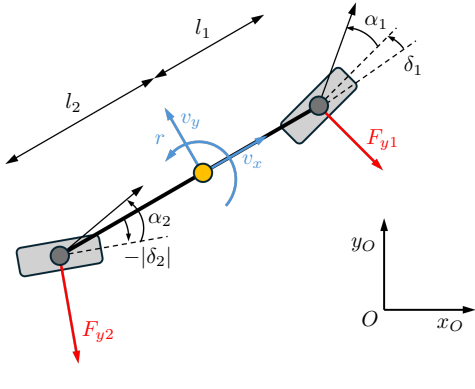


Figure 1: Single-track vehicle model. The kinematic variables are depicted in blue, the dynamic ones are in red.

puts, the linear ODE describing the rigid vehicle dynamics may be derived as [38]

$$\dot{v}_y(t) = -\frac{1}{m}(F_{y1}(t) + F_{y2}(t)) - v_x r(t), \quad (42a)$$

$$\dot{r}(t) = -\frac{1}{I_z}(l_1 F_{y1}(t) - l_2 F_{y2}(t)), \quad t \in (0, T), \quad (42b)$$

where the lumped states  $v_y(t)$ ,  $r(t) \in \mathbb{R}$  are the vehicle's lateral velocity and yaw rate,  $v_x \in \mathbb{R}_{>0}$  is its constant longitudinal speed,  $m \in \mathbb{R}_{>0}$  and  $I_z \in \mathbb{R}_{>0}$  denote respectively the vehicle mass and moment of inertia of the center of gravity around the vertical axis, and  $l_1, l_2 \in \mathbb{R}_{>0}$  are the front and rear axle lengths. Finally, adopting a distributed Dahl model for dry friction [10], the tire forces  $F_{y1}(t), F_{y2}(t) \in \mathbb{R}$  may be calculated as

$$F_{yi}(t) = L_i \int_0^1 p_i(\xi) \sigma_i z_i(\xi, t), \quad i \in \{1, 2\}, \quad (43)$$

where the distributed state  $z_i(\xi, t) \in \mathbb{R}$ ,  $i \in \{1, 2\}$ , represents the deflection of a bristle schematizing a tire rubber particle inside the contact patch,  $L_i \in \mathbb{R}_{>0}$  denotes the contact patch length,  $p_i \in C^1([0, 1]; \mathbb{R}_{\geq 0})$  is the vertical pressure distribution, and  $\sigma_i \in \mathbb{R}_{>0}$  is the normalized microstiffness coefficient [10]. The bristle dynamics is governed by the following PDE:

$$\begin{aligned} \frac{\partial z_i(\xi, t)}{\partial t} + \frac{v_x}{L_i} \frac{\partial z_i(\xi, t)}{\partial \xi} &= -\frac{\theta_i \sigma_i |v_i(v_y(t), r(t), \delta_i(t))|}{\mu_i(v_i(v_y(t), r(t), \delta_i(t)))} z_i(\xi, t) \\ &+ 2v_i(v_y(t), r(t), \delta_i(t)), \end{aligned} \quad (\xi, t) \in (0, 1) \times (0, T), \quad (44a)$$

$$z_i(0, t) = 0, \quad (44b)$$

where  $\theta_i \in \mathbb{R}_{>0}$  is the uncertain friction parameter,  $\mu_i \in C^1(\mathbb{R}; [\mu_{\min}, \infty))$ ,  $i \in \{1, 2\}$ , with  $\mu_{\min} \in \mathbb{R}_{>0}$ , is an expression for the nominal friction coefficient, and

$$v_1(v_y(t), r(t), \delta_1(t)) = v_y(t) + l_1 r(t) - v_x \delta_1(t), \quad (45a)$$

$$v_2(v_y(t), r(t), \delta_2(t)) = v_y(t) - l_2 r(t) - v_x \delta_2(t), \quad (45b)$$

being  $\delta_1(t), \delta_2(t) \in \mathbb{R}$  the steering inputs at the front and rear axles, respectively. Hence, defining  $\mathbb{R}^2 \ni X(t) \triangleq [v_y(t) \ r(t)]^T$ ,  $\mathbb{R}^2 \ni z(\xi, t) \triangleq [z_1(\xi, t) \ z_2(\xi, t)]^T$ ,  $\mathbb{R}^2 \ni U(t) \triangleq [\delta_1(t) \ \delta_2(t)]^T$ , and  $\mathbb{R}^2 \ni v(X(t), U(t)) = [v_1(X(t), U(t)) \ v_2(X(t), U(t))]^T \triangleq [v_1(v_y(t), r(t), \delta_1(t)) \ v_2(v_y(t), r(t), \delta_2(t))]^T$ , the resulting system may be recast in the form (1), with

$$\begin{aligned} A_1 &\triangleq \begin{bmatrix} 0 & -v_x \\ 0 & 0 \end{bmatrix}, \quad A_2 \triangleq \begin{bmatrix} 1 & l_1 \\ 1 & -l_2 \end{bmatrix}, \\ G_1 &\triangleq -\begin{bmatrix} \frac{1}{m} & \frac{1}{l_1} \\ \frac{m}{l_1} & \frac{m}{l_2} \end{bmatrix}, \quad G_2 \triangleq -v_x I_2, \\ K_1(\xi) &\triangleq \begin{bmatrix} L_1 \sigma_1 p_1(\xi) & 0 \\ 0 & L_2 \sigma_2 p_2(\xi) \end{bmatrix}, \quad A \triangleq \begin{bmatrix} \frac{v_x}{L_1} & 0 \\ 0 & \frac{v_x}{L_2} \end{bmatrix}, \\ \Sigma(v) &\triangleq \begin{bmatrix} -\frac{\sigma_1 |v_1|}{\mu_1(v_1)} & 0 \\ 0 & -\frac{\sigma_2 |v_2|}{\mu_2(v_2)} \end{bmatrix}, \quad h_2(v) \triangleq 2v, \end{aligned} \quad (46)$$

**Sym<sub>2</sub>(R)**  $\ni \Theta = \text{diag}\{\theta_1, \theta_2\}$ ,  $K_2 = K_3 = 0$ , and  $h_1(v) = 0$ . Finally, the vertical pressure distribution inside the tires' contact patches, appearing in (43) and (46), may be modeled using exponentially decreasing functions of the type [10]

$$p_i(\xi) = p_{0,i} \exp(-a_i \xi), \quad \xi \in [0, 1], \quad (47)$$

with  $p_{0,i}$ ,  $a_i \in \mathbb{R}_{>0}$ ,  $i \in \{1, 2\}$ .

The single-track model formulated according to (1), (46), and (47) may be used to estimate the friction coefficients at the front and rear axles,  $\theta_1$  and  $\theta_2$ , respectively, jointly with the vehicle states. Reliable information about tire-road friction is crucial not only for enhancing the internal performance of ADAS, but also to improve fleet and traffic flow coordination via vehicle-to-vehicle communication, and to support predictive operations such as road maintenance and salting [39, 40]. Starting with the measurements  $Y_1(t) = \frac{dz(0, t)}{dt}$  and  $Y_2(t) = \frac{d^2 z(0, t)}{dt^2}$ , which may be acquired using smart tire sensors mounted on both the front and rear axles, it is straightforward to verify that Assumption 2.2 holds for any combination of model parameters. In this context, it is perhaps worth mentioning that the yaw rate  $r(t)$  can be acquired with standard instrumentation equipped on any passenger vehicle, thus rendering one of the two boundary measurements redundant in most cases, especially if  $\theta_1 = \theta_2$  is assumed.

## 4.2 Simulation results

In the present section, the performance of the adaptive observer synthesized in Section 3.2 is evaluated considering the single-track model described by (1), and (46), (47).

The numerical values for the model parameters of the example discussed below are listed in Table 1.

With the given combination of parameters, the single-track model is understeer [38], and thus intrinsically stable for sufficiently low longitudinal speeds  $v_x$ , and small steering inputs  $\delta_1(t)$  and  $\delta_2(t)$ . The following results refer to

Parameter	Description	Unit	Value
$v_x$	Longitudinal speed	$\text{m s}^{-1}$	20
$m$	Vehicle mass	kg	1300
$I_z$	Vertical moment of inertia	$\text{kg m}^2$	2000
$l_1$	Front axle length	m	1
$l_2$	Rear axle length	m	1.6
$L_1$	Front contact patch length	m	0.11
$L_2$	Rear contact patch length	m	0.09
$\sigma_1$	Front micro-stiffness	$\text{m}^{-1}$	165
$\sigma_2$	Rear micro-stiffness	$\text{m}^{-1}$	415
$\mu_1(\cdot)$	Front nominal friction coefficient	-	1
$\mu_2(\cdot)$	Rear nominal friction coefficient	-	1
$p_{0,1}$	Front contact pressure at $\xi = 0$	$\text{N m}^{-1}$	$3.75 \cdot 10^4$
$p_{0,2}$	Rear contact pressure at $\xi = 0$	$\text{N m}^{-1}$	$2.86 \cdot 10^4$
$a_1$	Front pressure parameter	-	0.1
$a_2$	Rear pressure parameter	-	0.1

Table 1: Model parameters

numerical simulations conducted in MATLAB/Simulink<sup>®</sup> environment. The semilinear PDE subsystem was discretized in space using finite differences with a discretization step of 0.02, whereas the fixed time step was specified as  $10^{-6}$  s. The ICs for the actual system were set to  $X_0 = [3 - 0.4]^T$ , and  $z_0(\xi) = [0.3 0.3]^T$  (corresponding to  $\|z_0(\cdot)\|_{L^2((0,1); \mathbb{R}^2)} = 0.42$ ), whereas those for the observer to  $\dot{X}_0 = [0 0]^T$ ,  $\dot{z}_0(\xi) = [0 0]^T$ , and  $\mathbb{R}^2 \ni \hat{\theta}_0 \triangleq \hat{\theta}(0) = [0 0]^T$ . The observer gain  $L_1 \in \mathbf{M}_2(\mathbb{R})$  in (17) was specified as  $L_1 = -(A_1 + qI_2)A_2^{-1}$ , with  $q = 50$ ; the gains in (10), (13), and (14) were instead chosen as  $\varrho = 20$  and  $\psi = 50$ , and  $\Gamma = 5000I_2$ . Finally, a sinusoidal steering input, which is common in vehicle dynamics ([13, 14]), was designed with  $\delta_1(t) = 0.05 \sin(2t) + 0.01 \sin(4t)$  and  $\delta_2(t) = 0$ , and persistence of excitation was tested numerically.

Figure 2 illustrates the convergence of the parameter estimate  $\hat{\theta}(t)$  to the true value, corresponding to  $\theta = [1.2 0.8]^T$  for  $t < 5$  s, and to  $\theta = [0.6 0.4]^T$  for  $t \geq 5$  s. The abrupt change at  $t = 5$  s simulates a sudden discontinuity in friction, as might occur during a typical  $\mu$ -split maneuver. From Figure 2, it is evident that a good estimate of  $\theta$  is already achieved before  $t = 2$  s during the first phase; during the second phase, the convergence is reached around  $t = 8$  s. Due to the presence of the absolute value  $|\cdot|$  in (44) and in the matrix  $\Sigma(v)$  in (46), the source term is intrinsically non-smooth. Hence, the convergence of the observer error states should be investigated in the norm  $\|(\tilde{X}(t), \tilde{z}(\cdot, t))\|_{\mathcal{X}}$ . In particular, the theoretical predictions of Theorem 3.2 were also corroborated in simulation, as demonstrated graphically in Figure 3, where the norms  $\|(X(t), z(\cdot, t))\|_{\mathcal{X}}$ ,  $\|(\tilde{X}(t), \tilde{z}(\cdot, t))\|_{\mathcal{X}}$ , and  $\|(\tilde{X}(t), \tilde{z}(\cdot, t))\|_{\mathcal{X}}$  are plotted together ( $t \leq 2$  s). A satisfactory estimate of the lumped and distributed states is achieved around

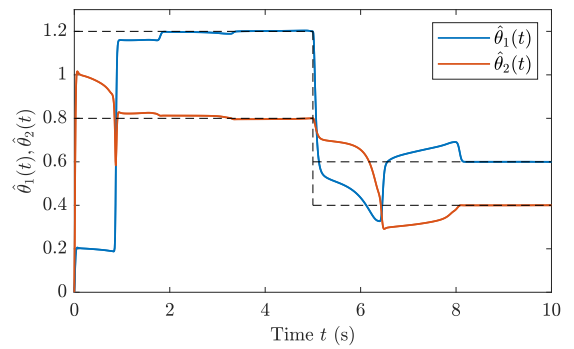


Figure 2: Convergence of the parameter estimate  $\hat{\theta}(t)$  to the true value  $\theta$ .

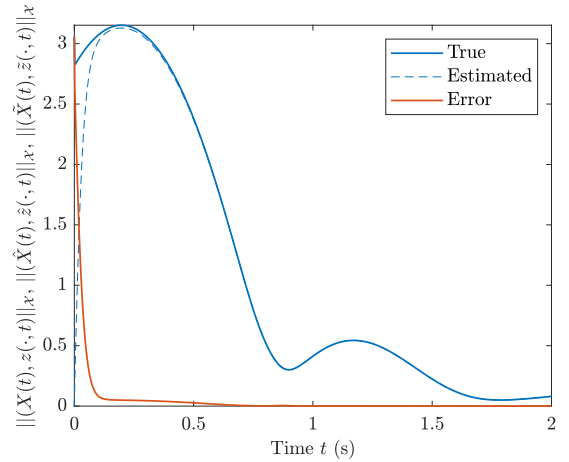


Figure 3: True states (solid tick blue line), observer estimates (dotted blue line), and observer error (solid orange line).

$t = 0.25$  s, as indicated by the rapid initial decrease of  $\|(\tilde{X}(t), \tilde{z}(\cdot, t))\|_{\mathcal{X}}$  to a value near zero. Subsequently, the error remains extremely small, and only exhibits a minor transient after the abrupt change in friction occurring at  $t = 5$  s, as shown in Figure 4. A more detailed visualization of the distributed error dynamics is offered in Figure 5, which shows the evolution of  $\tilde{z}_1(\xi, t)$  for  $t \leq 2$  s. The conclusions that may be drawn by inspection of Figure 5 are consistent with the observations reported above. The trend of the variable  $\tilde{z}_2(\xi, t)$  is similar and omitted for brevity.

Finally, it should be emphasized that the proposed observer for the PDE variables relies on exact cancellation via transport dynamics. To evaluate the robustness of the approach, additional simulations were performed by replacing the true transport velocity in (17b) with an estimate obtained using a deliberately mismatched longitudinal speed,  $\hat{v}_x = 0.8v_x$ . The results, omitted here due to space restrictions, confirmed that the observer maintains satisfactory performance in the presence of significant parameter uncertainty.

## 5 Conclusion

This paper focused on the synthesis of an adaptive observer for a class of semilinear ODE-PDE systems representing mechanical systems with distributed friction and rolling contact dynamics. Specifically, a boundary-sensing-based observer was designed that achieves joint estimation of both the lumped and distributed states, as well as uncertain friction parameters. Under persistence of excitation conditions, theoretical guarantees of convergence were provided for both mild and classical solutions, and validated through simulations on a vehicle dynamics benchmark. Future work will focus on experimental validation and extension to bidirectional PDE systems and multi-contact configurations.

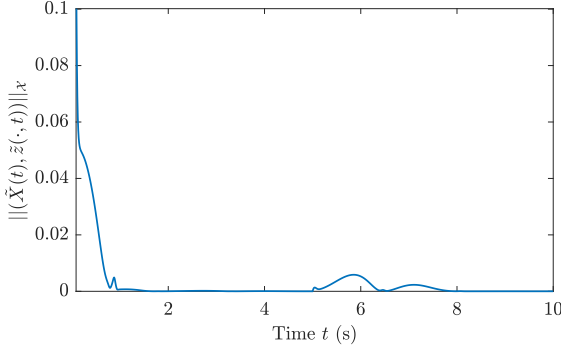


Figure 4: Convergence of the observer error estimate.

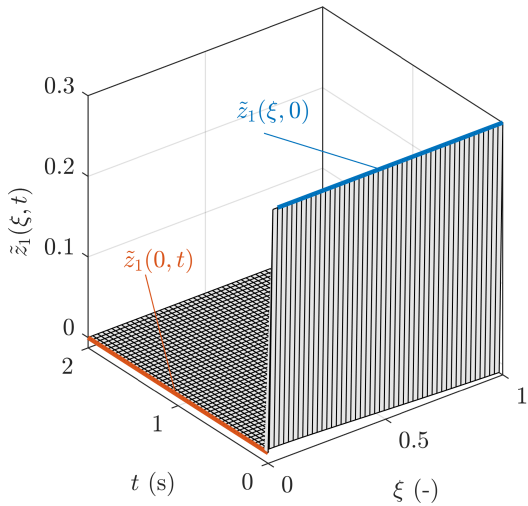


Figure 5: Evolution of the PDE error state  $\tilde{z}_1(\xi, t)$ , along with its IC (blue line) and BC (orange line).

## Acknowledgments

This research was financially supported by the project FASTEST (Reg. no. 2023-06511), funded by the Swedish Research Council.

## References

- [1] C. Canudas de Wit and P. Tsotras (1999). Dynamic tire friction models for vehicle traction control, Proc. IEEE Conf. Dec. Contr., Phoenix, AZ, USA, 4, 3746-3751.
- [2] C. Canudas-de-Wit, P. Tsotras, E. Velenis, et al. (2003). Dynamic Friction Models for Road/Tire Longitudinal Interaction, Veh. Syst. Dyn. 39(3), 189-226.
- [3] E. Velenis, P. Tsotras, C. Canudas-de-Wit and M. Sorine (2005). Dynamic tyre friction models for combined longitudinal and lateral vehicle motion, Veh Syst Dyn 43(1), 3-29.
- [4] J. Deur, J. Asgari and D. Hrovat (2004). A 3D Brush-type Dynamic Tire Friction Model, Veh. Syst. Dyn., 42(3), 133-173.
- [5] J. Deur, V. Ivanović, M. Troulis, et al. (2005). Extensions of the LuGre tyre friction model related to variable slip speed along the contact patch length, Veh. Syst. Dyn., 43(sup.1), 508-524.
- [6] L. Romano, F. Bruzelius and B. Jacobson (2022). An extended LuGre-brush tyre model for large camber angles and turning speeds, Veh. Syst. Dyn., 61(6), 1674-1706.
- [7] F. Frendo and F. Bucchi (2020). "Brush model" for the analysis of flat belt transmissions in steady-state conditions, Mechanism and Machine Theory, 143, 103698.
- [8] F. Frendo and F. Bucchi (2020). Enhanced brush model for the mechanics of power transmission in flat belt drives under steady-state conditions: Effect of belt elasticity, Mechanism and Machine Theory, 153, 104003.
- [9] G. A. Waltersson and Y. Karayannidis (2024). Planar Friction Modeling With LuGre Dynamics and Limit Surfaces, IEEE Transactions on Robotics, 40, 3166-3180.
- [10] L. Romano, O. M. Aamo, J. Åslund and E. Frisk (in press). Stability and dissipativity of the distributed LuGre friction model, IEEE Contr. Syst. Lett.
- [11] L. Romano, O. M. Aamo, J. Åslund and E. Frisk (2025). First-order friction models with bristle dynamics: lumped and distributed formulations, submitted to IEEE Transactions on Contr. Syst. Tech.
- [12] M. Tanelli, A. Astolfi and S. M. Savarese (2008). Robust nonlinear output feedback control for brake by wire control systems, Automatica, 44(4), 1078-1087.
- [13] L. Shao, C. Jin, C. Lex and A. Eichberger (2016). Nonlinear adaptive observer for side slip angle and road friction estimation, IEEE Trans. Autom. Control, 61(10), 3250-3256.

tion, Proc. IEEE Conf. Dec. Contr. (CDC), Las Vegas, NV, USA, 6258-6265.

[14] L. Shao, C. Jin, C. Lex et al (2019). Robust road friction estimation during vehicle steering, *Veh. Syst. Dyn.*, 57(4), 493-519.

[15] A. Smyshlyaev and M. Krstic (2010). Adaptive control of parabolic PDEs, 1st ed., Princeton University Press.

[16] P. Bernard and M. Krstic (2014). Adaptive output-feedback stabilization of non-local hyperbolic PDEs, *Automatica*, 50(10), 2692-2699.

[17] H. Anfinsen and O. M. Aamo (2019). Adaptive Control of Hyperbolic PDEs, 1st ed., Springer Cham.

[18] O. M. Aamo (2013). Disturbance rejection in  $2 \times 2$  linear hyperbolic systems, *IEEE Trans. Auto. Contr.*, 58(5), 1095-1106.

[19] M. Ghosein and E. Witrant (2023). Adaptive observer design for uncertain hyperbolic PDEs coupled with uncertain LTV ODEs; Application to refrigeration systems, *Automatica*, 154, 111233.

[20] A. Benabdellahi, F. Giri, T. Ahmed-Ali, et al. (2021). Adaptive observer design for wave PDEs with nonlinear dynamics and parameter uncertainty, *Automatica*, 123, 109331.

[21] H. Anfinsen and O. M. Aamo (2022). Leak detection, size estimation and localization in branched pipe flows, *Automatica*, 140, 110109.

[22] H. Anfinsen, M. Diagne, O. M. Aamo et al. (2016). An Adaptive Observer Design for  $n + 1$  Coupled Linear Hyperbolic PDEs Based on Swapping, *IEEE Trans. Auto. Contr.*, 61(12), 3979-3990.

[23] H. Anfinsen and O. M. Aamo (2017). State estimation in hyperbolic PDEs coupled with an uncertain LTI system, Proc. American Contr. Conf. (ACC), Seattle, WA, USA, 3821-3827.

[24] J. Wu, J. Zhan and L. Zhang (2024). Adaptive Boundary Observers for Hyperbolic PDEs With Application to Traffic Flow Estimation, *IEEE Trans. Auto. Contr.*, 69(1), 651-658.

[25] L. Zhang, J. Wu and J. Zhan (2024). Adaptive observer design for coupled ODE-hyperbolic PDE systems with application to traffic flow estimation, *Automatica*, 167, 111033.

[26] A. Hasan, O. M. Aamo and M. Krstic (2016). Boundary observer design for hyperbolic PDE-ODE cascade systems, *Automatica*, 68, 75-86.

[27] H. Anfinsen and O. M. Aamo (2017). Estimation of Parameters in a Class of Hyperbolic Systems with Uncertain Transport Speeds, Proc. Med. Conf. Contr. Auto. (MED), Valletta, Malta.

[28] H. Anfinsen, H. Holta and O. M. Aamo (2020). Adaptive Control of a Linear Hyperbolic PDE with Uncertain Transport Speed and a Spatially Varying Coefficient, Proc. Med. Conf. Contr. Auto. (MED), Saint-Raphaël, France, 945-951.

[29] G. Bastin and J.-M. Coron (2016). Stability and Boundary Stabilization of 1-D Hyperbolic Systems, 1st ed., Birkhäuser Cham.

[30] T. Kato (1995). Perturbation Theory for Linear Operators, 2nd ed., Springer Berlin, Heidelberg.

[31] L. Romano, O. M. Aamo, J. Åslund and E. Frisk (2025). Semilinear single-track vehicle models with distributed tyre friction dynamics, *Nonlinear Dyn.*

[32] C. Canudas-de-Wit and R. Horowitz (1999). Observers for tire/road contact friction using only wheel angular velocity information, Proc. IEEE Conf. Dec. Contr. (CDC), Phoenix, AZ, USA, 4, 3932-3937.

[33] G. Rill, T. Schaeffer and M. Schuderer (2024). LuGre or not LuGre, *Multibody System Dynamics*, 60, 191-218.

[34] F. Marques, P. Flores, J. C. Pimenta Claro, et al. (2016). A survey and comparison of several friction force models for dynamic analysis of multibody mechanical systems, *Nonlinear Dyn.*, 86, 1407-1443.

[35] F. Marques, L. Woliński, M. Wojtyra, et al. (2021). An investigation of a novel LuGre-based friction force model, *Mechanism and Machine Theory*, 166, 104399.

[36] P. Ioannou and J. Sun (1995). Robust Adaptive Control, Prentice-Hall, Inc., Upper Saddle River, NJ, USA.

[37] L. Romano, O. M. Aamo, J. Åslund and E. Frisk (2025). Stability and stabilization of semilinear single-track vehicle models with distributed tire friction dynamics via singular perturbation analysis, submitted to *Automatica*.

[38] M. Guiggiani (2023). The Science of Vehicle Dynamics, 3rd ed., Springer International, Cham.

[39] M. Wielitzka, M. Dagen and T. Ortmaier (2017). State and maximum friction coefficient estimation in vehicle dynamics using UKF, Proc. American Contr. Conf. (ACC), Seattle, WA, USA, 4322-4327.

[40] A. Albinsson, F. Bruzelius, B. Jacobson and J. Fredriksson (2016). Design of tyre force excitation for tyre-road friction estimation, *Veh. Syst. Dyn.*, 55(2), 208-230.

[41] A. Pazy (1983). Semigroups of Linear Operators and Applications to Partial Differential Equations, 1st ed., Springer New York, NY.

## A Proof of Lemma 3.1

The proof of Lemma 3.1 is given below.

*Proof of Lemma 3.1.* Consider the transformations  $\mathbb{R}^{n_x} \ni W(t) \triangleq \tilde{X}(t)e^{-\rho t}$ ,  $\mathbb{R}^{n_x} \ni W^n(t) \triangleq \tilde{X}^n(t)e^{-\rho t}$ ,  $\mathbb{R}^{n_z} \ni w(\xi, t) \triangleq \tilde{z}(\xi, t)e^{-\rho t}$ , and  $\mathbb{R}^{n_z} \ni w^n(\xi, t) \triangleq \tilde{z}^n(\xi, t)e^{-\rho t}$ , with  $\rho \in \mathbb{R}_{>0}$  to be determined. Substitution into (21) and (24) yields respectively the two ODE-PDE systems:

$$\dot{W}(t) = -\rho W(t) + \bar{A}_1 W(t) + G_1(\mathcal{K}_1 w)(t) + F_1(t)(\mathcal{K}_2 w)(t) + f_1(t), \quad t \in (0, T), \quad (48a)$$

$$\frac{\partial w(\xi, t)}{\partial t} + \Lambda \frac{\partial w(\xi, t)}{\partial \xi} = -\rho w(\xi, t) + F_2(t)w(\xi, t) + f_2(\xi, t), \quad (\xi, t) \in (0, 1) \times (0, T), \quad (48b)$$

$$w(0, t) = 0, \quad t \in (0, T), \quad (48c)$$

and

$$\dot{W}^n(t) = -\rho W^n(t) + \bar{A}_1 W^n(t) + G_1(\mathcal{K}_1 w^n)(t) + F_1^n(t)(\mathcal{K}_2 w^n)(t) + f_1^n(t), \quad t \in (0, T), \quad (49a)$$

$$\frac{\partial w^n(\xi, t)}{\partial t} + \Lambda \frac{\partial w^n(\xi, t)}{\partial \xi} = -\rho w^n(\xi, t) + F_2^n(t)w^n(\xi, t) + f_2^n(\xi, t), \quad (\xi, t) \in (0, 1) \times (0, T), \quad (49b)$$

$$w^n(0, t) = 0, \quad t \in (0, T), \quad (49c)$$

It is straightforward to verify that, for  $\rho \in \mathbb{R}_{>0}$  large enough, the unbounded operator  $(\mathcal{A}_\rho, \mathcal{D}(\mathcal{A}_\rho))$ , defined by

$$(\mathcal{A}_\rho(Y, v)) \triangleq \begin{bmatrix} -\rho Y + \bar{A}_1 Y + G_1(\mathcal{K}_1 v) \\ -\Lambda \frac{\partial v(\xi)}{\partial \xi} - \rho v(\xi) \end{bmatrix}, \quad (50a)$$

$$\mathcal{D}(\mathcal{A}_\rho) \triangleq \{(Y, v) \in \mathcal{Y} \mid v(0) = 0\}, \quad (50b)$$

satisfies  $\mathcal{A}_\rho \in \mathcal{G}(\mathcal{X}; 1, -\omega_\rho)$ , where  $\omega_\rho \in \mathbb{R}_{>0}$  may be made arbitrarily large by increasing  $\rho$ . Denoting by  $T_{\mathcal{A}_\rho}(t)$ ,  $t \in [0, T]$ , the  $C_0$ -semigroup generated by  $\mathcal{A}_\rho$ , in the abstract setting, for all ICs  $(W_0, w_0) \triangleq (W(0), w(\cdot, 0)) \in \mathcal{X}$  and  $(W_0^n, w_0^n) \triangleq (W^n(0), w^n(\cdot, 0)) \in \mathcal{X}$ , the mild solutions of (48) and (49) read respectively ([41], Chapter 6)

$$\begin{bmatrix} W(t) \\ w(t) \end{bmatrix} = T_{\mathcal{A}_\rho}(t) \begin{bmatrix} \tilde{X}_0(t) \\ \tilde{z}_0(t) \end{bmatrix} + \int_0^t T_{\mathcal{A}_\rho}(t-t') \times \left( F(t) \begin{bmatrix} W(t') \\ w(t') \end{bmatrix} + f(t') \right) dt', \quad (51a)$$

$$\begin{bmatrix} W^n(t) \\ w^n(t) \end{bmatrix} = T_{\mathcal{A}_\rho}(t) \begin{bmatrix} \tilde{X}_0^n(t) \\ \tilde{z}_0^n(t) \end{bmatrix} + \int_0^t T_{\mathcal{A}_\rho}(t-t') \times \left( F^n(t) \begin{bmatrix} W^n(t') \\ w^n(t') \end{bmatrix} + f^n(t') \right) dt', \quad t \in [0, T], \quad (51b)$$

where  $f, f^n : \mathcal{X} \times [0, T] \mapsto \mathcal{X}$ , with  $\mathbb{R}^{nx+nz} \ni f(\xi, t) \triangleq [f_1^\top(t) \ f_3^\top(\xi, t)]^\top$  and  $\mathbb{R}^{nx+nz} \ni f^n(\xi, t) \triangleq [f_1^{n\top}(t) \ f_3^{n\top}(\xi, t)]^\top$ , and

$$F(t) \triangleq \begin{bmatrix} F_1(t) & 0 \\ 0 & F_2(t) \end{bmatrix}, \quad F^n(t) \triangleq \begin{bmatrix} F_1^n(t) & 0 \\ 0 & F_2^n(t) \end{bmatrix}. \quad (52)$$

Defining  $\mathbb{R}^{nx} \ni \tilde{W}^n(t) \triangleq W(t) - W^n(t)$  and  $\mathbb{R}^{nz} \ni \tilde{w}^n(\xi, t) \triangleq w(\xi, t) - w^n(\xi, t)$ , subtracting (51b) from (51a), and using the fact that  $\mathcal{A}_\rho \in \mathcal{G}(\mathcal{X}; 1, -\omega_\rho)$  yields

$$\begin{aligned} \left\| (\tilde{W}^n(t), \tilde{w}^n(\cdot, t)) \right\|_{\mathcal{X}} &\leq e^{-\omega_\rho t} \left\| (\tilde{W}_0^n, \tilde{w}_0^n(\cdot)) \right\|_{\mathcal{X}} \\ &+ \frac{\|F(\cdot)\|_\infty}{\omega_\rho} \left\| (\tilde{W}^n(\cdot), \tilde{w}^n(\cdot, \cdot)) \right\|_\infty \\ &+ \frac{\left\| (W^n(\cdot), w^n(\cdot, \cdot)) \right\|_\infty}{\omega_\rho} \|F(\cdot) - F^n(\cdot)\|_\infty \\ &+ \frac{1}{\omega_\rho} \|f(\cdot, \cdot) - f^n(\cdot, \cdot)\|_\infty, \quad t \in [0, T], \end{aligned} \quad (53)$$

where  $\mathcal{X} \ni (\tilde{W}_0^n, \tilde{w}_0^n(\xi)) \triangleq (\tilde{W}^n(0), \tilde{w}^n(\xi, 0))$ , and

$$\left\| (W^n(\cdot), w^n(\cdot, \cdot)) \right\|_\infty \triangleq \sup_{t \in \mathbb{R}_{\geq 0}} \left\| (W^n(t), w^n(\cdot, t)) \right\|_{\mathcal{X}}, \quad (54a)$$

$$\left\| (\tilde{W}^n(\cdot), \tilde{w}^n(\cdot, \cdot)) \right\|_\infty \triangleq \sup_{t \in \mathbb{R}_{\geq 0}} \left\| (\tilde{W}^n(t), \tilde{w}^n(\cdot, t)) \right\|_{\mathcal{X}}. \quad (54b)$$

Theorem 3.2 ensures that  $\left\| (W^n(\cdot), w^n(\cdot, \cdot)) \right\|_\infty$  is bounded for  $t \in \mathbb{R}_{\geq 0}$ , and  $\|F(\cdot)\|_\infty$  exists and is bounded by assumption. Since  $\omega_\rho \in \mathbb{R}_{>0}$  may be selected arbitrarily to satisfy  $\omega_\rho > \|F(\cdot)\|_\infty$ , the above inequality (53) implies the existence of a constant  $\beta_\rho \in \mathbb{R}_{>0}$  such that

$$\begin{aligned} \left\| (\tilde{W}^n(\cdot), \tilde{w}^n(\cdot, \cdot)) \right\|_\infty &\leq \beta_\rho \left( \left\| (\tilde{W}_0^n, \tilde{w}_0^n(\cdot)) \right\|_{\mathcal{X}} \right. \\ &\left. + \|F(\cdot) - F^n(\cdot)\|_\infty + \|f(\cdot, \cdot) - f^n(\cdot, \cdot)\|_\infty \right), \quad t \in [0, T]. \end{aligned} \quad (55)$$

Letting  $n \rightarrow \infty$  in (55) and recalling (25) provides (27).  $\square$